Physical-chemical properties of non-soluble particles in a hailstone collected in Argentina

A. C. Bernal Ayala[1], A. K. Rowe[1], L. E. Arena[2,3], W. O. Nachlas[4]

[1]Department of Atmospheric and Oceanic Sciences, University of Wisconsin, Madison, WI, USA
[2]Facultad de Matemáticas, Astronomía, Física y Computación, Universidad Nacional de Córdoba, Córdoba, Argentina
[3]Observatorio Hidrometereológico de Córdoba, Córdoba, Argentina
[4]Department of Geoscience, University of Wisconsin, Madison, WI, USA

Key Points:

- Hailstones near Cordoba, Argentina, show diverse carbonaceous particles, with the largest particles located at center of the hailstone.
- Silicate and carbonaceous particles coexist within the same hailstone layers, originating from soil and agricultural sources.
- Anthropogenic activities contribute to heavy metals in hailstones, emphasizing the need to consider urban influences in aerosol modeling.

Corresponding author: Anthony Crespo Bernal Ayala, crespo3@wisc.edu

Abstract

This study presents a novel analysis of a hailstone collected near Cordoba, Argentina, quantifying the composition, size distribution, and potential sources of non-soluble particles contained within. The hailstone contained diverse particles, with sizes ranging from 1.9 to 150.3 µm, primarily carbonaceous, including in the center, suggesting a possible biological and geological influence on hail formation. Silicate particles were distributed throughout the hailstone, likely from eroded soil and agricultural activities. Finally, salts were detected in the outer layers of the hailstone and may have originated from the nearby salt lake. This study highlights the regional influence of various land use types on hail formation and growth and points to the potential impacts of natural and anthropogenic factors on hailstone composition.

Plain Language Summary

In this study, scientists investigated hailstones collected in Argentina to understand the particles trapped inside them and their potential impact on hail formation. Hailstorms cause significant damage and economic losses, and understanding how hailstones form is crucial. A unique method was used in this project to analyze the hailstones without melting them, revealing the size, composition, and origin of particles within an individual hailstone.

The hailstone contained various types of particles, mostly carbon-based, possibly from biological and geological sources. Silicate particles, originating from eroded soil and agricultural activities, were also present, suggesting that local winds carried these particles into the clouds where hail formed.

The research highlights the importance of local environmental factors, such as land use, in influencing the composition of hailstones. The findings contribute to our understanding of the complex processes involved in hail formation and shed light on the potential impacts of both natural and human-related factors on hailstone composition. This study opens the door for further research on hailstones collected in different environmental conditions, providing valuable insights for future studies and potential applications in weather forecasting and risk assessment.

1 Introduction

Falling hailstones are destructive natural phenomena contributing to billion-dollar disasters in the U.S. (Changnon, 2008; Sander et al., 2013; Allen et al., 2017; Kumjian et al., 2019) and significant agricultural losses globally (Calori et al., 2016; Streifeneder et al., 2023). Understanding hail formation, including its environmental controls and variations within storm modes, has been limited owing to challenges in validating remotely sensed proxies (Cecil & Blankenship, 2012; Bang & Cecil, 2019; Bruick et al., 2019) and studying hail growth globally (e.g., Allen et al. 2020). Aerosols ingested into convective cloud updrafts are known to serve as hail embryos via heterogeneous nucleation, either through frozen cloud drops initially forming on cloud condensation nuclei (CCN) or rimed ice crystals forming on non-soluble ice nucleating particles (INP); however, the effects of CCN and INP on hail formation remain largely inconclusive from modeling studies (Fan et al., 2013; Lebo & Morrison, 2014).

Previous research has used collected hailstones to examine the role of environmental aerosols, CCN, and INPs in hail formation and found links to local land use. For example, biological ice nuclei were found in hailstone embryos in the U.S. Rocky Mountains (Michaud et al., 2014), while hailstones collected in Slovenia (Šantl-Temkiv et al., 2013) and the triple border region of Paraguay, Brazil, and Argentina (Beal et al., 2021) noted signatures of the respective regions' soil. Others point to anthropogenic markers

through the presence of microplastics (Kozjek et al., 2023), highlighting the implications of human activity on hail formation. The analysis techniques in those studies all required melting the hailstones, removing information on particle size distribution or composition with respect to the hailstone embryo, necessarily neglecting non-soluble particles, or both. This present work, using a new method (Bernal Ayala, Rowe, Arena, Nachlas, & Asar, 2024) to address several limitations of previous work, aims to gain a more comprehensive understanding of hailstones' composition and inferred microphysical processes through analysis of non-soluble particles contained within hailstones.

This study analyzes a 4 *cm* hailstone collected near Cordoba, Argentina (Fig. 1; lime green star), an area known for its intense hail-producing storms (Zipser et al., 2006; Cecil & Blankenship, 2012; Rasmussen et al., 2014; Bernal Ayala et al., 2022) and the focus of recent collaborative field campaigns: the 2018-19 Cloud, Aerosol, and Complex Terrain Interactions (CACTI) (Varble, 2021) and the 2018 Remote Sensing of Electrification, Lightning, and Mesoscale/Microscale Processes with Adaptive Ground Observations (RELAMPAGO) (Nesbitt et al., 2021). A survey of INPs collected at the surface over the Sierras de Córdoba (SDC; Fig. 1) during CACTI (Testa et al., 2021) found that diverse plant communities in the region release high amounts of biological particles and intensively farmed areas contribute organic soil dust, indicating their potential role in hail formation via INPs. The hailstone in this analysis formed from an isolated supercell that developed at 1700 UTC on 8 February 2018 on the northern section of the SDC (red star in Fig. 1) that did not feature large-scale environmental conditions typical of widespread convection in this region (Rasmussen & Houze, 2016), thus suggesting a local, regional influence on storm formation (Bernal Ayala et al., 2022). We, therefore, hypothesize a contribution from both biological and soil-derived particulates to hail formation and growth in this event. This study is the first to characterize the elemental composition of particles in their original spatial context within the hailstone interior. Using a novel application of microscopy-based methods for hailstone analysis (Bernal Ayala, Rowe, Arena, Nachlas, & Asar, 2024), this study addresses the following questions: 1) What is the particle size and spatial distribution of non-soluble particles trapped within the hailstone sample? 2) What are the major element compositions of the non-soluble particles from different regions of the hailstone? 3) Which land use regions are potential sources of the non-soluble particles identified in the hailstone?

2 Data and Methods

2.1 Hailstone Collection and Preparation

The 8 February hailstone was collected by residents of Villa Carlos Paz (VCP; lime green star, Fig.1) through contact with Dr. Lucia Arena at the Facultad de Matemática, Astronomía, Física y Computación at the Universidad Nacional de Córdoba "FAMAF-UNC" and the COSECHEROS Program (*Cosecheros de granizo Córdoba*, 2022). Collected hailstones were processed at the FAMAF-UNC's subzero facility, Laura Levi Atmospheric Physics Laboratory. Once cut, hailstones were sublimated and coated with a specific polyvinyl formal (FORMVAR) solution diluted in ethylene dichloride to trap the particles within the hailstone layers. More details on the hailstone collection and preparation are provided in Bernal Ayala, Rowe, Arena, Nachlas, and Asar (2024).

2.2 Microscopy analysis and elemental characterization

The unique microscopy technique for analysis is detailed in Bernal Ayala, Rowe, Arena, Nachlas, and Asar (2024) and summarized here. The technique is based on the method of separating insoluble particles by adapted sublimation (Arena, 2023), which involves covering a thin sheet of hail, approximately 1*mm* thick, with a 1% FORMVAR solution to promote sublimation at below-zero temperatures to capture particles beneath the plastic film. Once the ice has sublimated, the particles can be studied at room tem-

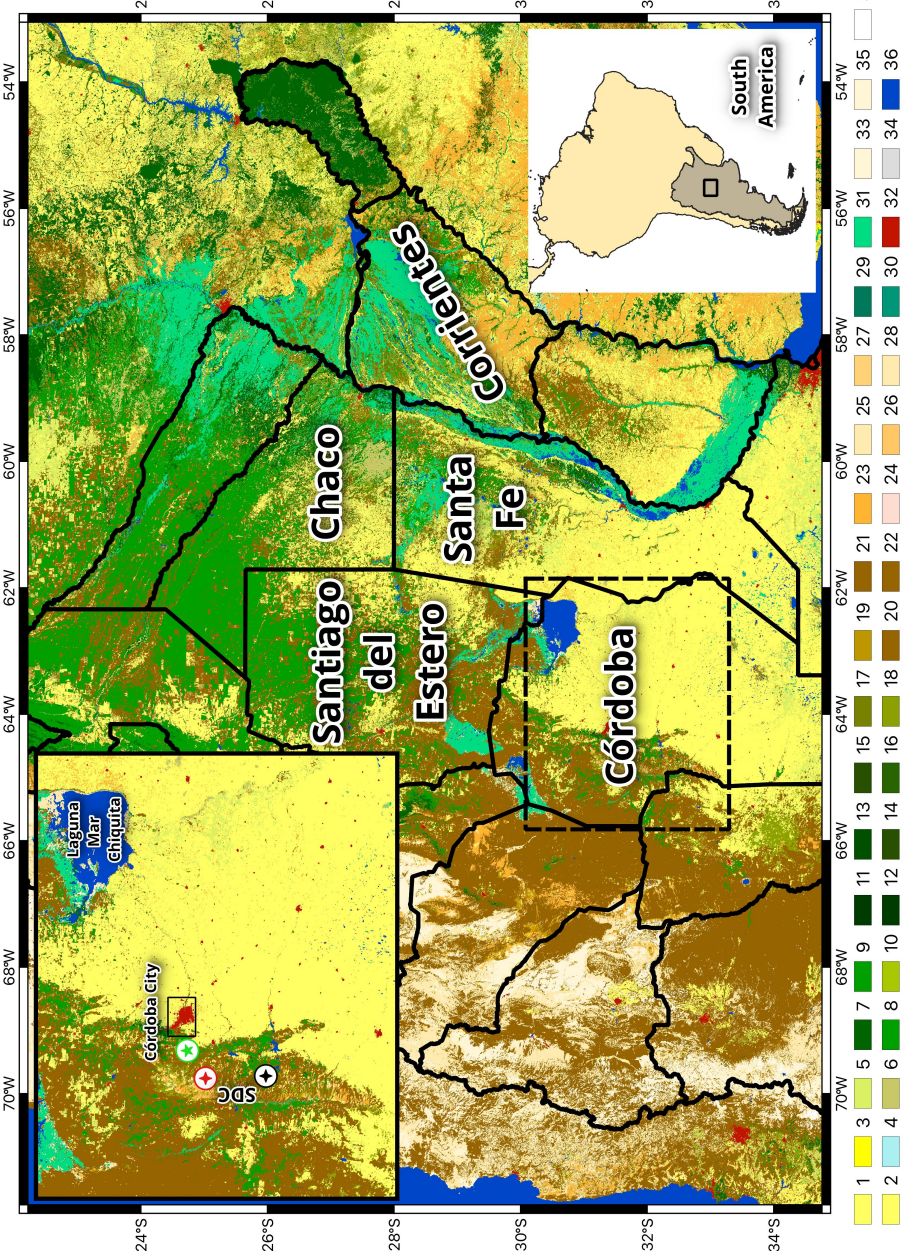

Figure 1. Map of northern Argentina covering an area shown in the black box in the lower right panel, including the Córdoba study area and nearby provinces. Within the dashed box covering northern Córdoba province is an inset (top left) highlighting Córdoba City to the east of the Sierras de Córdoba (SDC) and points of interest for this analysis: the site of the CACTI experiment observations in Villa Yacanto (black star), the hail collection location (lime green star), and the initiation point of the hail-producing cell (red star). Color fill represents the C3S Land Cover map available through the C3S Climate Data Store (CDS): 1-cropland rainfed, 2-cropland rainfed, 3-cropland rainfed tree or shrub cover, 4-cropland irrigated, 5-mosaic cropland, 6-mosaic natural vegetation, 6-tree broadleaved evergreen closed to open, 7-tree broadleaved deciduous closed to open, 8-tree broadleaved deciduous closed, 9-tree broadleaved deciduous open, 10-tree needleleaved evergreen closed to open, 11-tree needleleaved evergreen closed, 12-tree needleleaved evergreen open, 13-tree needleleaved deciduous closed to open, 14-tree needleleaved deciduous closed, 15-tree needleleaved deciduous open, 16-tree mixed, 17-mosaic tree and shrub, 18-mosaic herbaceous, 19-shrubland, 20-shrubland evergreen, 21-shrubland deciduous, 22-grassland, 23-lichens and mosses, 24-sparse vegetation, 25-sparse tree, 26-sparse shrub, 27-sparse herbaceous, 28-tree cover flooded fresh or brackish water, 29-tree cover flooded saline water, 30-shrub or herbaceous cover flooded, 31-urban, 32-bare areas, 33-bare areas consolidated, 34-bare areas unconsolidated, 35-water, 36-snow and ice.

perature. This novel approach applies microscopy techniques more frequently used in other disciplines, such as Geology (Hurley et al., 2021; Han et al., 2022), to uniquely provide information on non-soluble particle physical and chemical characteristics with respect to the hailstone center. A 2-D cross-section of the hail sample was created using an OLYMPUS LEXT OLS4000 Confocal Laser Scanning Microscope (CLSM), using the embryo as a reference and then scanning the sample from both ends. Within this area, sectors were selected for further magnification to identify individual particles manually with respect to the hailstone embryo. ProfilmOnline was used to calculate particle size. This detailed approach provided particle size distribution for 76 identified particles within this 4 cm hailstone, including particles as small as 1 μm within individual sectors of the 2-D cross-section.

The sublimated hailstone sample was gold-coated and analyzed using a ZEISS FEG-SEM Σigma Scanning Electron Microscope (SEM-EDS) with backscatter and secondary electron images created at $15kV$ and $8.5mm$ working distance. Manual SEM particle examination confirmed 73 of the original 76 particles from CLSM analysis for further physical-chemical analysis. To avoid interference with the sample substrate, EDS spectra were acquired from the center of each particle using a single-point analysis technique to determine the elemental composition of individual particles. The following elements were identified, with abundance $\geq 1\%$ by weight (C, N, O, F, Na, Mg, Al, Si, S, Cl, K, Ca, Ti, Cr, Fe, Ni, Zn, Br, Mo), with elements $\geq 10\%$ considered predominant. Finally, a large area elemental cross-section was acquired at 0.8 μm resolution across a diameter of the equatorial plane to evaluate the elemental distribution throughout the hailstone sample, providing insights into the overall composition distribution from the center (e.g., embryo or nuclei).

2.3 Air Mass Trajectories

The NOAA Air Resources Laboratory's Hybrid Single-Particle Lagrangian Integrated Trajectory model (HYSPLIT)(Stein et al., 2015) was used to generate a 24-hour air mass back-trajectory using European Environment Agency Reanalysis data sets (ERA5) (Hersbach et al., 2020), with a vertical resolution of 37 pressure levels: $25hPa$ from 1025 through $750hPa$, $50hPa$ from 750 through $300hPa$, and $25hPa$ from 275 through $100hPa$. These trajectories were initiated at 1700 UTC with hourly intervals, starting at unique model heights of 100 (first pressure level above surface), 500 and 1000 (boundary-layer variability), and (d) 1500 (low-level jet level) meters AGL from the convective core coordinates [-64.75,-31.59] identified at initiation time using channel 11 (8.4 μm) from the geostationary satellite GOES-16 (Bernal Ayala et al., 2022). A trajectory matrix with a 7x5 grid with 0.3 spacing was also processed from the initial point and time for five days to investigate any path variations for an air parcel before convective initiation. The area covered by all back-trajectories was divided into grid cells with dimensions of 0.28 longitude and 0.28 latitude (i.e., ERA-5 horizontal resolution). Each trajectory occurrence in each grid cell was normalized based on the time spent over each grid, including trajectory endpoints for all the heights (Ashbaugh et al., 1985). Residence-time coefficient pixels were then compared with the 22-class C3S Climate Data Store Land Cover classification gridded map from 2023 (e.g., Fig. 1). This approach provides insight into the highest probability of a specific land use being a source region for the non-soluble particles analyzed in this study.

3 Results

3.1 Particle Size and Elemental Composition of Individual Particles

The CLSM analysis of the 73 individual particles revealed maximum particle sizes ranging from 1.9 to 150.3 μm with a precision uncertainty of ± 0.2 μm (Fig. 2) and an average particle size of 40 μm. These sizes were larger on average than particles found

in the CACTI INP study (Testa et al., 2021) in Villa Yacanto, Argentina (black star in Fig. 1), which analyzed ground-based INP measurements from instrumentation capable of measuring sizes only up to 20 μm. While particles of up to 100 μm are likely to remain suspended in the atmosphere for up to 2 days (Jaenicke, 1978; Bakan et al., 1987), the larger particles observed here, up to 150 μm, suggest that intense local winds were required to loft those particles into the cloud. Overall, the greatest size variability is observed in particles trapped in the center of the hailstone.

To evaluate if those size differences are owing to particle composition, the 73 identified particles were characterized based on elemental weight percentages from the SEM-EDS analysis (Laskin et al., 2012) using the statistical-based Orange's k-means characterization method with silhouette scores (Demšar et al., 2013). Based on the outcomes derived from the particle classification output of the k-means analysis, alongside the awareness that EDS alone is incapable of distinguishing between biological and non-biological species, we systematically categorized the particles into five general groups: Carbonaceous (e.g., Fig. 3, A), Carbonaceous with heavy metals, Silicates (e.g., Fig. 3, B), Silicates with heavy metals, and Salts (e.g., Fig.3, C). Particles included in the Carbonaceous group contained C greater than 10 % and greater than Cl and Si weight percentages. Particles in the Silicates group had Si greater than 10 % and greater than C and Cl. Particles containing Cl greater than 10 % and greater than C and Si were categorized in the Salts group.

This classification scheme revealed that the particles in the hailstone were primarily carbonaceous (66%; Fig. 2), containing carbon either in the inorganic, organic, or elemental form that can be from anthropogenic, biological, or geological origin. Of the carbonaceous particles, 19% contained heavier metals such as Br, Fe, Ni, Mo, Ti, and Cr, with weight percentages individually greater than 1%. Regardless of whether these carbonaceous particles contained heavy metals, they were spread throughout the hailstone with no apparent higher concentration in any one layer relative to the center. The carbonaceous particles also contained the largest particle size with the highest size variability ranging from 5 to 150 μm with no preferential size distribution throughout the sample. The second most prevalent group was particles categorized in the Silicates group. This group composed 22% of all particles with size variability ranging from 2 to 55 μm (Fig. 2). Similar to the carbonaceous group, silicate particles were spread through the sample, and no apparent maximum concentration or size was observed in layers with respect to the center. A subsidiary category to Silicates was Silicates with heavier metals, which only composed 4% of the sample, with sizes from 11 to 45 μm. These samples had at least 10% of Silicon as particles in the Silicates group. Still, these particles contained Br and Fe with weight percentages individually greater than 1% and were found in the outer layers of the hailstone. Lastly, Salt particles compose 8% of the entire sample. Salt particle sizes range from 8 to 29 μm (Fig. 2), primarily concentrated in the outer layers of the hailstone. The full 2-D chemical cross section (Fig. 4) confirmed the presence of C throughout the sample. Si was challenging to distinguish due to glass interference. Finally, high Cl concentrations indicated the presence of salt particles in the hailstone's outer layers (Fig. 4 bottom), as revealed in the analysis of randomly selected individual particles, but also near the center of the hailstone (Fig. 4 top).

3.2 Possible Source Regions

The analysis of the 24-hour HYSPLIT back trajectory (Fig. 5, A, top) sheds light on the possible origins of the particles in the hailstone sample with distinct patterns at different altitude levels. Levels 100 and 500 m AGL come initially from the northwest but then loop over the northeastern part of the SDC, likely owing to the upslope flow of surface winds from the north and northeast (Bernal Ayala et al., 2022). This upslope flow is supported by the terrain and height change of the wind, moving upslope supported by the terrain analysis seen in Fig. 5, A (bottom figure). The 1000 and 1500 m trajec-

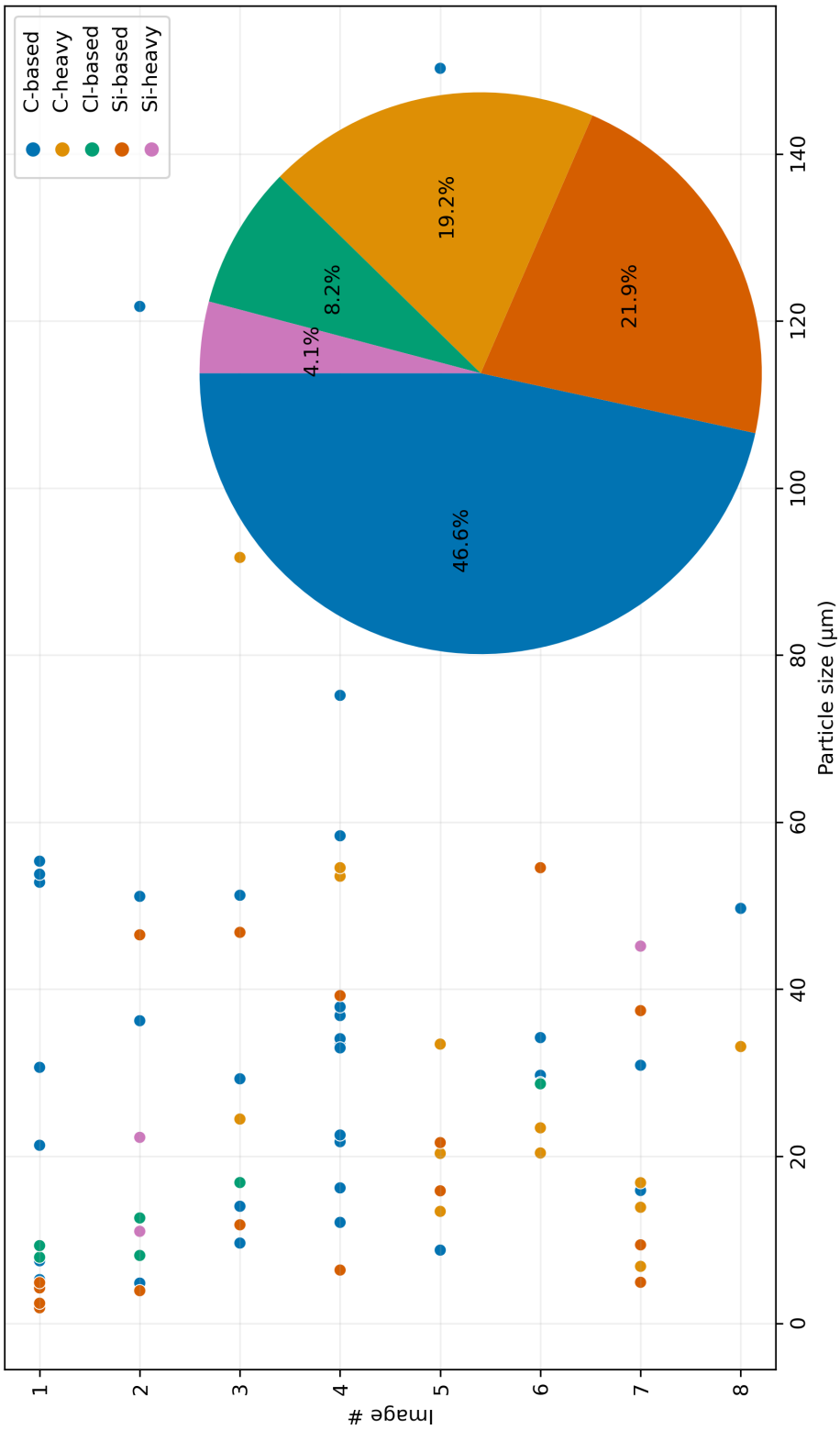

Figure 2. Particle size distribution graph (X-axis in μm) through the cross-section of the hailstone along a diameter of the equatorial plane (Y-axis in μm), with 0 and 8 representing the outermost layers of the hailstone, and images 4 and 5 depicting the center of the hailstone. The pie chart insert illustrates the elemental composition percentages of the 76 identified particles within the $4cm$ hailstone with colors corresponding to those used in the particle size distribution plot.

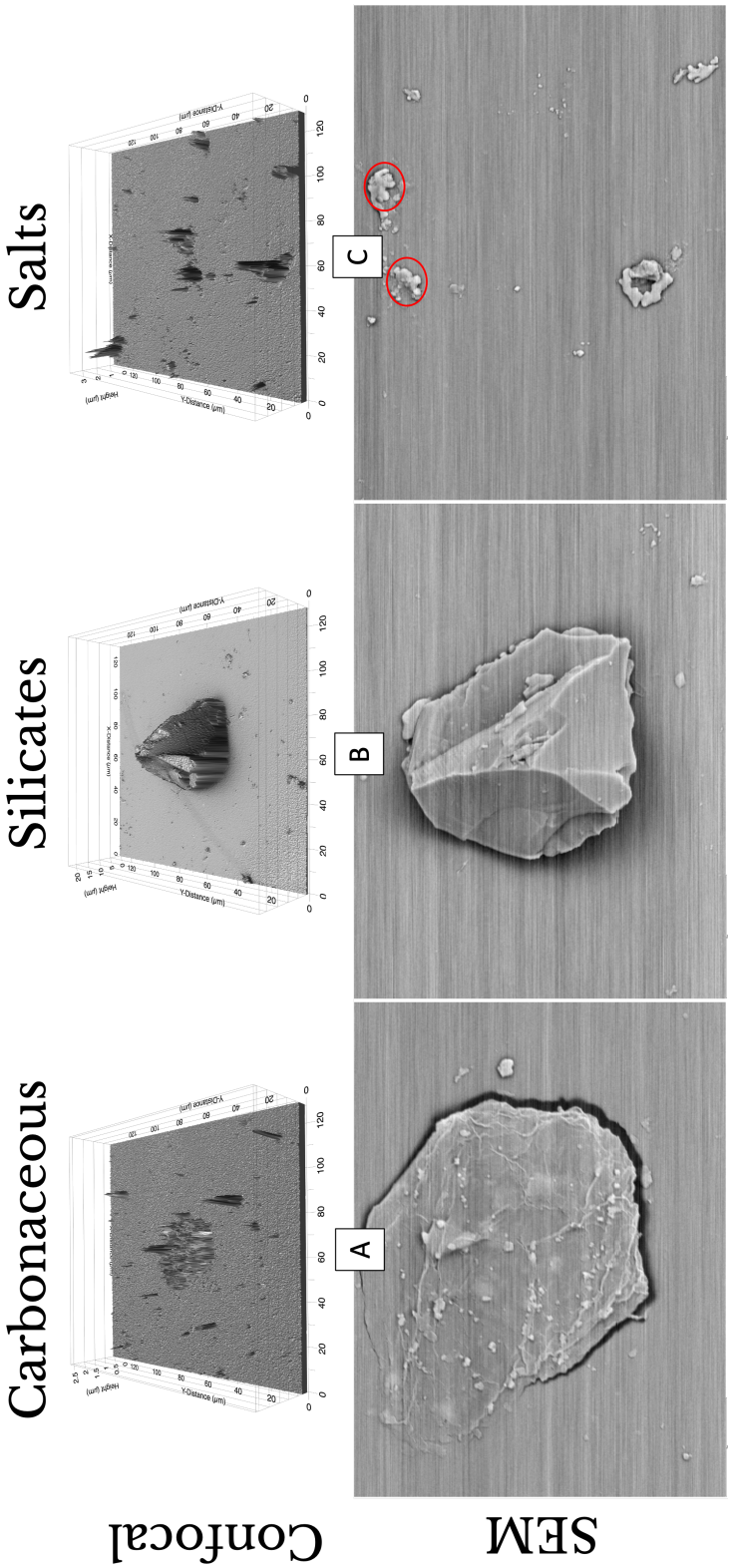

Figure 3. Examples from each of the primary particle categories are presented, along with their ProFilmOnline topographical output obtained through a Confocal Laser Scanning Microscope (CLSM, top), accompanied by their corresponding Scanning Electron Microscopy (SEM, bottom) image.

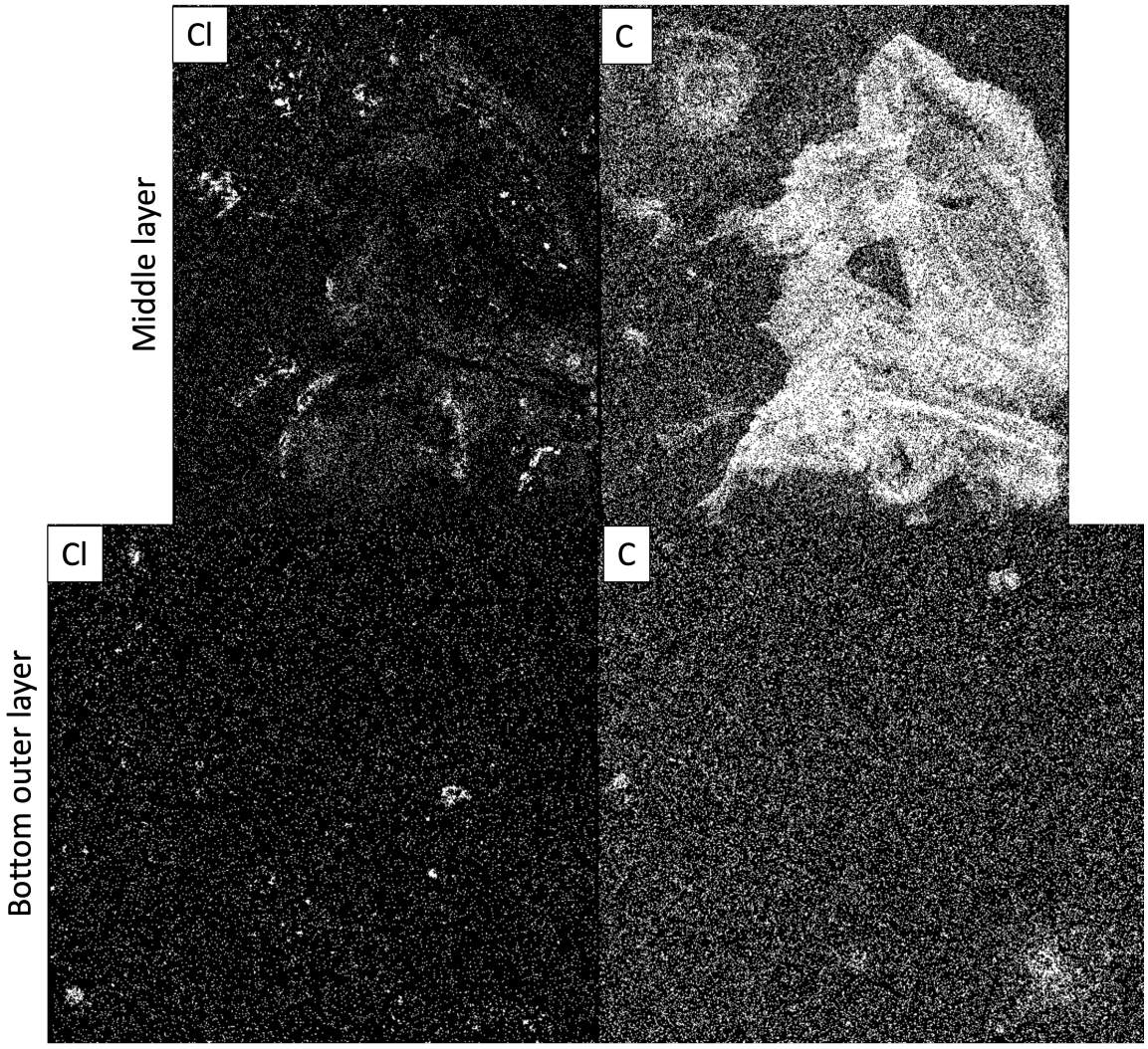

Figure 4. 2-D EDS cross-section of the complete hailstone sample processed in Fiji-ImageJ V2.14.0. This cross-section illustrates the intensity of elements Cl and C, with brighter spots indicating higher concentrations. Middle layers are positioned between images 4 and 5 in Figure 2, while the outer layers are situated between images 7 and 8.

tories initially come from the north and northwest, then show a slight curvature north of the Cordoba Province and later from the northeast. The residence time coefficients calculated for 5-day back-trajectories (Fig. 5, B) similarly highlight the regional influence. Under the assumption that the particles arriving at the location where the hail-producing storm initiated are more likely emitted from regions where the air masses spent more time (Yadav et al., 2021; Ren et al., 2021; Testa et al., 2021), the grid cells showing the high residence-time coefficients are considered potentially principal sources for the particles found in the hailstone. The regions with the highest residence-time coefficients (orange, yellow, and red in Fig. 5, B) are generally located over the SDC, Cordoba City, Argentina's largest natural salt lake (Laguna Mar Chiquita), and Provinces such as Santiago del Estero, Chaco, Santa Fe, and Corrientes (Fig. 1). These results reveal that discernible sources only within Argentina's geographical limits account for possible non-soluble particulate sources in the analyzed hailstone sample, supporting Bernal Ayala et al. (2022)'s conclusion of local environmental factors responsible for this case. Furthermore, in comparing the residence-time coefficient pixels from the 5-day back trajectory with the C3S Land Cover map (Fig. 5, B), we find the most predominant land uses (Fig. 5, C) showing high residence-time coefficient areas are Shrublands, Croplands, areas covered by Mixed Vegetation, Urban areas (mostly Cordoba city), and areas with a body of water (the Salt Lake), consistent with the findings of carbonaceous, mineral, and salt particles, as well as heavy metals, throughout the hailstone.

4 Discussion

Our results show, for the first time, the sizes, composition, and distribution with respect to the stone's center of non-soluble particles trapped in a hailstone in Argentina. This analysis reveals the presence of carbonaceous particles within the embryo of the hailstone, consistent with the prevalence of biological particles in this region (Testa et al., 2021) and the presence of carbonaceous particles near the center of the hailstones in other parts of the world (Šantl-Temkiv et al., 2013; Michaud et al., 2014; Beal et al., 2021). Additionally, observations of carbonaceous particles up to 150 μm in diameter suggest the influence of strong local winds, which effectively suspended these larger particles for a sufficient time, enabling them to be entrained within the updraft. These results reinforce the important role of biological and geological particles in understanding hail formation in deep convective clouds globally.

Silicates were also detected near the hailstone's center with particle sizes ranging from 7 to 39 μm, overlapping with the carbonaceous particle size ranges. These silicates can be attributed to eroded particles from the surrounding mountains, specifically K-feldspar commonly found in agricultural topsoil, as well as soil dust particles resulting from agricultural activities in this region (Testa et al., 2021). The identification of larger silicate particles in the center of the hailstone suggests that they were sufficiently large to nucleate at temperatures similar to those of the carbonaceous particles, aligning with the findings of Beal et al. (2021). Among the mineral particles, K-feldspar has previously been identified as the most ice-active component for promoting ice nucleation (Kiselev et al., 2017). When compared to pure mineral standards, the coexistence of Na, Cl, Mg, Ca, and various elements within the silicate particles in our sample suggests the aggregation of particles with multiple mineral phases. This finding aligns with the notion that when silicates become suspended in the air, they can potentially aggregate with other atmospheric particles, resulting in the coagulation of compositions that enhance their nucleation potential. This effect is particularly pronounced at higher temperatures, as Pruppacher and Klett (1980) indicated.

Regarding the outer layer of the hailstone, we observed a consistent size distribution encompassing various groups of particle composition, including carbonaceous particles that were evenly distributed throughout the sample. Within this outer layer, we detected smaller silicate particles that may have been too small to act as INPs during

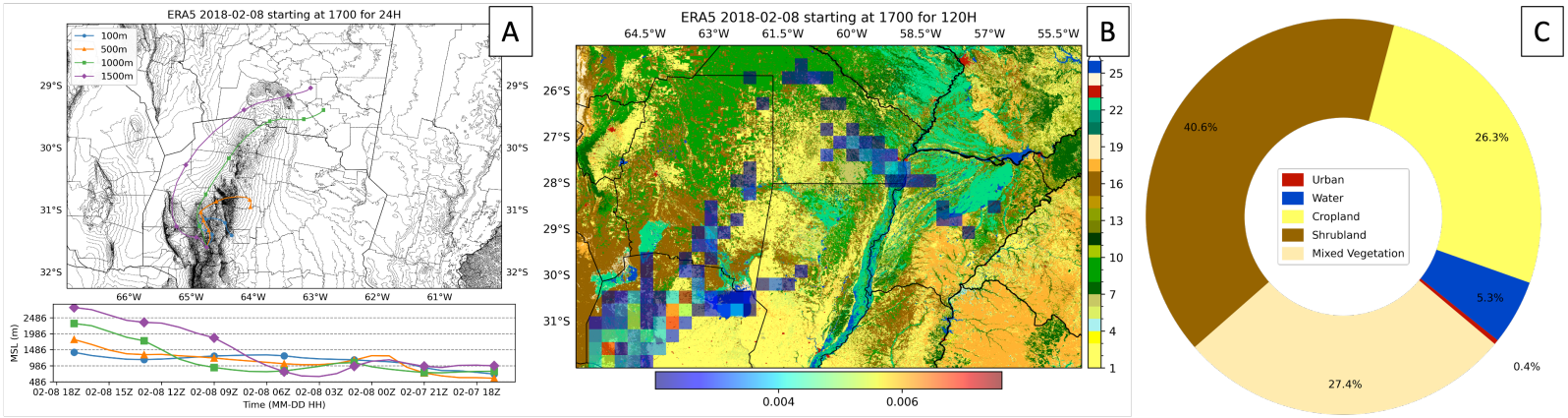

Figure 5. Figure A (top) shows 24-hour HYSPLIT back trajectories color-coded by height (in meters), as the legend defines. The bottom part of Figure A displays terrain analysis in meters above sea level for the same time periods as the back trajectories. Figure B shows residence time coefficients calculated for 5-day back trajectories overlaid on the C3S Land Cover map. The land cover colors correspond to a subset of categories shown in Figure 1, specifically: 1/2/3-Cropland rain-fed, 4-Cropland irrigated, 5-Mosaic cropland, 6-Mosaic natural vegetation, 7-Evergreen broadleaved, 8/9/10-Deciduous broadleaved, 11-Evergreen needleleaved, 12-Mixed trees, 13-Mosaic tree/shrub, 14-Mosaic herbaceous, 15/16-Shrubland, 17-Grassland, 18-Sparse vegetation, 19-Sparse herbaceous, 20-Fresh water flooded tree cover, 21- Saline water flooded tree cover, 22-Flooded shrub/herbaceous cover, 23-Urban, 24-Bare areas, 25-Water, 26-Snow and ice. Figure C displays the predominant land uses within the residence time coefficient pixels observed in Figure B. Similar land uses were grouped into the following categories: Urban (23), Water (25,26), Cropland(1,2,3,4,5), Shrubland(15,16,17), Mixed Vegetation (6,7,8,9,10,11,12,13,14,18,19). Flooded Vegetation (20,21,22) and bare areas (24) were not included.

the formation of the hailstone embryo. Still, they could have served as CCN and accumulated onto the hailstone during phases when the temperature allowed for the accumulation of supercooled liquid water, thereby continuing the growth of the hailstone layers. Additionally, we detected salts in the hailstone, which likely originated from particles acting as CCN. This result suggests that the salts, potentially originating from the salt lake northeast of the SDC, could mix with other atmospheric particles, potentially leading to an increased presence of insoluble CCNs during hailstone growth.

The SEM-EDX analysis revealed that 12 of the 73 analyzed particles contained heavier metals such as Br, Fe, Ni, Ti, Mo, and Cr, most combined with silicates and biological particles. Anthropogenic sources may contribute to the presence of heavier metals in the particles (Beal et al., 2021), which has implications for modeling aerosol interactions. Therefore, considering the influence of anthropogenic activities in nearby urban areas is essential, as they may transport heavier metals that may mix with other silicates and carbon-based particles suspended in the atmosphere. Additionally, they can be absorbed by surrounding vegetation, which can subsequently re-emit them back into the atmosphere (Pruppacher & Klett, 1980). These metals later become available to mix with other atmospheric particles, potentially affecting ice nucleation temperatures within the cloud.

5 Conclusions

Using a novel technique described in Bernal Ayala, Rowe, Arena, Nachlas, and Asar (2024), this study provides first-of-their-kind insights into the composition, size distribution, and potential sources of non-soluble particles within a hailstone collected near Cordoba, Argentina. The results indicate that the hailstone contains diverse particles, with carbonaceous particles dominating the hailstone sample, including the embryo, with silicate and salt particles distributed throughout the sample. The presence of carbonaceous particles suggests a strong influence of biological and geological sources in hail formation, while silicates originate from eroded soil particles and agricultural activities. The particle size distribution, particularly the detection of larger particles up to 150 μm, points to the role of local winds in lofting particles into the convective cloud, where they could participate in nucleation and growth processes.

This study highlights the regional influence of various land use types, including shrublands, croplands, urban areas, and bodies of water, specifically a salt lake. It supports the idea that local environmental factors play a significant role in the particles in the hailstone. Overall, this study enhances our understanding of the complex interplay between land-use sources emitting atmospheric particles, local environmental conditions, and hailstone formation processes. The findings contribute to ongoing research in hail formation and offer insights into the potential impacts of natural and anthropogenic factors on the elemental chemical composition of hailstones. Future work will analyze additional hailstones collected in this region under different environmental conditions.

6 Open Research Section

The physical (CLSM) and chemical (EDS) data of hailstones are stored in an Excel sheet, which has been uploaded and is accessible through Zenodo (Bernal Ayala, Rowe, Arena, & Nachlas, 2024). We obtained the ERA5 reanalysis data from Hersbach et al. (2023) and the land cover classification gridded map from the Copernicus Climate Change Service, Climate Data Store Service (2019). This ERA5 data was input to the National Oceanographic and Atmospheric Administration's Hybrid Single-Particle Lagrangian Integrated Trajectory (HYSPLIT) model (version 5.3.0) (available at https://www.ready.noaa.gov/HYSPLIT.php) to produce residence time coefficient plots based on the air mass trajectories.

Acknowledgments

This research was supported by the National Science Foundation (grants AGS-1640452 and AGS-2146708). Thank you to Sebastian García for his assistance at LAMARX-UNC and Maria L. Asar for her contributions to developing the method used in this paper.

References

Allen, J. T., Tippett, M. K., Kaheil, Y., Sobel, A. H., Lepore, C., Nong, S., & Muehlbauer, A. (2017). An Extreme Value Model for U.S. Hail Size. *Monthly Weather Review*, *145*(11), 4501–4519. doi: 10.1175/MWR-D-17-0119.1

Arena, L. E. (2023, July). Identificación de partículas incluidas en hielos naturales (glaciares, permafrost, granizo) por sublimación adaptada.

Ashbaugh, L. L., Malm, W. C., & Sadeh, W. Z. (1985). A residence time probability analysis of sulfur concentrations at grand Canyon national park. *Atmospheric Environment*, *19*, 1263–1270.

Bakan, S., Hinzpeter, H., Höller, H., Jaenicke, R., Jeske, H., Laube, M., ... Wurzinger, C. (1987). *Physical and chemical properties of the air / physikalische und chemische eigenschaften der luft* (Vol. 4 Sub Vol B). Springer Berlin Heidelberg.

Bang, S. D., & Cecil, D. J. (2019, September). Constructing a Multifrequency Passive Microwave Hail Retrieval and Climatology in the GPM Domain. *Journal of Applied Meteorology and Climatology*, *58*(9), 1889–1904. doi: 10.1175/JAMC-D-19-0042.1

Beal, A., Martins, L. D., Martins, J. A., Rudke, A. P., de Almeida, D. S., Costa, L. M., & Tarley, C. R. T. (2021). Evaluation of the chemical composition of hailstones from triple border Paraná, Santa Catarina (Brazil) and Argentina. *Atmospheric Pollution Research*, *12*(3), 184–192. doi: 10.1016/j.apr.2021.01.009

Bernal Ayala, A. C., Rowe, A., Arena, L. E., & Nachlas, W. O. (2024, January). *Individual Particle Dataset: Physical-chemical properties of non-soluble particles in a hailstone collected in Argentina.* Zenodo. (Funding by National Science Foundation ROR 021nxhr62.) doi: https://doi.org/10.5281/zenodo.10455803

Bernal Ayala, A. C., Rowe, A. K., Arena, L. E., & Desai, A. R. (2022). Evaluation of Satellite-Derived Signatures for Three Verified Hailstorms in Central Argentina. *Meteorology*, *1*(2), 183–210. doi: 10.3390/meteorology1020013

Bernal Ayala, A. C., Rowe, A. K., Arena, L. E., Nachlas, W. O., & Asar, M. L. (2024). Revolutionizing Hailstone Analysis: Exploring Non-Soluble Particles through Innovative Confocal Laser and Scanning Electron Microscopy Techniques. *Atmos. Meas. Tech.*. doi: (Under-review)

Bruick, Z. S., Rassumen, K. L., & Cecil, D. J. (2019, December). Subtropical South American Hailstorm Characteristics and Environments. *Mon. Weather Rev.*, *147*, 4289–4304. doi: 10.1175/MWR-D-19-0011.1

Calori, A., Santos, J. R., Blanco, M., Pessano, H., Llamedo, P., Alexander, P., & de la Torre, A. (2016, July). Ground-based GNSS network and integrated water vapor mapping during the development of severe storms at the Cuyo region (Argentina). *Atmospheric Research*, *176–177*, 267–275. doi: 10.1016/j.atmosres.2016.03.002

Cecil, D. J., & Blankenship, C. B. (2012, January). Toward a Global Climatology of Severe Hailstorms as Estimated by Satellite Passive Microwave Imagers. *JCLI*, *25*, 687–703. doi: 10.1175/JCLI-D-11-00130.1

Changnon, S. A. (2008). Temporal and Spatial Distributions of Damaging Hail in the Continental United States. *Physical Geography*, *29*(4), 341–350. doi: 10.2747/0272-3646.29.4.341

Cosecheros de granizo Córdoba. (2022, August). https://www.argentina.gob.ar/ciencia/sact/ciencia-ciudadana/cosecheros-de-granizo-cordoba.

Demšar, J., Curk, T., Erjavec, A., Gorup, Č., Hočevar, T., Milutinovič, M., ... Zupan, B. (2013, January). Orange: Data Mining Toolbox in Python. *J. Mach. Learn. Res.*, *14*(1), 2349–2353.

Fan, J., Leung, L. R., Rosenfeld, D., Chen, Q., Li, Z., Zhang, J., & Yan, H. (2013). Microphysical effects determine macrophysical response for aerosol impacts on deep convective clouds. *Proceedings of the National Academy of Sciences*, *110*(48), E4581-E4590. doi: 10.1073/pnas.1316830110

Han, S., Löhr, S. C., Abbott, A. N., Baldermann, A., Farkaš, J., McMahon, W., ... Owen, M. (2022). Earth system science applications of next-generation SEM-EDS automated mineral mapping. *Frontiers in Earth Science*, *10*.

Hersbach, H., Bell, B., Berrisford, P., Biavati, G., Horányi, A., Muñoz-Sabater, J., ... Thépaut, J.-N. (2023). *ERA5 hourly data on pressure levels from 1940 to present.* Copernicus Climate Change Service (C3S) Climate Data Store (CDS). doi: 10.24381/cds.bd0915c6

Hersbach, H., Bell, B., Berrisford, P., Hirahara, S., Horányi, A., Muñoz-Sabater, J., ... Thépaut, J.-N. (2020). The ERA5 global reanalysis. *Quarterly Journal of the Royal Meteorological Society*, *146*(730), 1999–2049. doi: 10.1002/qj.3803

Hurley, N. F., Nakamura, K., & Rosenberg, H. (2021, July). Microporosity quantification using confocal microscopy. *Journal of Sedimentary Research*, *91*(7), 735–750. doi: 10.2110/jsr.2020.030

Jaenicke, R. (1978, January). Physical properties of atmospheric particulate sulfur compounds. *Atmospheric Environment (1967)*, *12*(1), 161–169. doi: 10.1016/0004-6981(78)90197-X

Kiselev, A., Bachmann, F., Pedevilla, P., Cox, S. J., Michaelides, A., Gerthsen, D., & Leisner, T. (2017). Active sites in heterogeneous ice nucleation—the example of K-rich feldspars. *Science*, *355*(6323), 367–371. doi: 10.1126/science.aai8034

Kozjek, M., Vengust, D., Radošević, T., Žitko, G., Koren, S., Toplak, N., ... Viršek, M. K. (2023, January). Dissecting giant hailstones: A glimpse into the troposphere with its diverse bacterial communities and fibrous microplastics. *Sci Total Environ*, *856*(Pt 1), 158786. doi: 10.1016/j.scitotenv.2022.158786

Kumjian, M. R., Lebo, Z. J., & Ward, A. M. (2019). Storms Producing Large Accumulations of Small Hail. *Journal of Applied Meteorology and Climatology*, *58*(2), 341–364. doi: 10.1175/JAMC-D-18-0073.1

Laskin, A., Moffet, R. C., Gilles, M. K., Fast, J. D., Zaveri, R. A., Wang, B., ... Shutthanandan, J. (2012). Tropospheric chemistry of internally mixed sea salt and organic particles: Surprising reactivity of NaCl with weak organic acids. *Journal of Geophysical Research: Atmospheres*, *117*(D15). doi: 10.1029/2012JD017743

Lebo, Z. J., & Morrison, H. (2014). Dynamical Effects of Aerosol Perturbations on Simulated Idealized Squall Lines. *Monthly Weather Review*, *142*(3), 991–1009. doi: 10.1175/MWR-D-13-00156.1

Michaud, A. B., Dore, J. E., Leslie, D., Lyons, W. B., Sands, D. C., & Priscu, J. C. (2014). Biological ice nucleation initiates hailstone formation. *J. Geophys. Res. Atmos.*, *119*, 12,186–12,197. doi: 10.1002/2014JD022004

Nesbitt, S. W., Salio, P. V., Ávila, E., Bitzer, P., Carey, L., Chandrasekar, V., ... Grover, M. A. (2021). A Storm Safari in Subtropical South America: Proyecto RELAMPAGO. *Bulletin of the American Meteorological Society*, *102*(8), E1621 - E1644. doi: 10.1175/BAMS-D-20-0029.1

Pruppacher, H. R., & Klett, J. D. (1980). *Microphysics of Clouds and Precipitation* (Vol. 18). Springer Netherlands.

Rasmussen, K. L., & Houze, R. A., Jr. (2016, May). Convective Initiation near the Andes in Subtropical South America. *Monthly Weather Review*, *144*(6), 2351–2374. doi: 10.1175/MWR-D-15-0058.1

Rasmussen, K. L., Zuluaga, M. D., & Houze Jr., R. A. (2014). Severe convection and lightning in subtropical South America. *Geophysical Research Letters*, *41*(20), 7359–7366. (doi: 10.1002/2014GL061767) doi: 10.1002/2014GL061767

Ren, L., Yang, Y., Wang, H., Wang, P., Chen, L., Zhu, J., & Liao, H. (2021). Aerosol transport pathways and source attribution in China during the COVID-19 outbreak. *Atmospheric Chemistry and Physics*, *21*(20), 15431–15445. doi: 10.5194/acp-21-15431-2021

Sander, J., Eichner, J. F., Faust, E., & Steuer, M. (2013). Rising Variability in Thunderstorm-Related U.S. Losses as a Reflection of Changes in Large-Scale Thunderstorm Forcing. *Weather, Climate, and Society*, *5*(4), 317–331. doi: 10.1175/WCAS-D-12-00023.1

Šantl-Temkiv, T., Finster, K., Dittmar, T., Hansen, B. M., Thyrhaug, R., Nielsen, N. W., & Karlson, U. G. (2013, January). Hailstones: A Window into the Microbial and Chemical Inventory of a Storm Cloud. *PLOS ONE*, *8*(1), 1–7. doi: 10.1371/journal.pone.0053550

Service, C. C. C. (2019). *Land cover classification gridded maps from 1992 to present derived from satellite observation. Copernicus Climate Change Service (C3S) Climate Data Store (CDS).* doi: 10.24381/cds.006f2c9a

Stein, A. F., Draxler, R. R., Rolph, G. D., Stunder, B. J. B., Cohen, M. D., & Ngan, F. (2015). NOAA's HYSPLIT Atmospheric Transport and Dispersion Modeling System. *Bulletin of the American Meteorological Society*, *96*(12), 2059–2077. doi: 10.1175/BAMS-D-14-00110.1

Streifeneder, V., Hölbling, D., & Dabiri, Z. (2023, February). *Impact of hail events on agriculture: A remote sensing-based analysis of hail damage in the context of climate change* (Tech. Rep. No. EGU23-2551). Copernicus Meetings. doi: 10.5194/egusphere-egu23-2551

Testa, B., Hill, T. C. J., Marsden, N. A., Barry, K. R., Hume, C. C., Bian, Q., ... DeMott, P. J. (2021). Ice Nucleating Particle Connections to Regional Argentinian Land Surface Emissions and Weather During the Cloud, Aerosol, and Complex Terrain Interactions Experiment. *Journal of Geophysical Research: Atmospheres*, *126*(23), e2021JD035186. (e2021JD035186 2021JD035186) doi: 10.1029/2021JD035186

Varble, A. (2021). Utilizing a storm-generating hotspot to convective cloud transitions: The CACTI experiment. *Bull. Amer. Met. Soc.*

Yadav, S. K., Kompalli, S. K., Gurjar, B. R., & Mishra, R. K. (2021). Aerosol number concentrations and new particle formation events over a polluted megacity during the COVID-19 lockdown. *Atmospheric Environment*, *259*, 118526. doi: 10.1016/j.atmosenv.2021.118526

Zipser, E. J., Nesbitt, S. W., Liu, C., & Yorty, D. P. (2006, August). Where Are the Most Intense Thunderstorms on Earth? *B AM METEOROL SOC*, 1057–1071. doi: 10.1175/BAMS-87-8-1057